Optimal process parameters for 3D printing of dental porcelain structures

Hadi Miyanaji[a], Shanshan Zhang[a], Austin Lassell[a], Amir Ali Zandinejad[b], Li Yang[a]

[a]Department of Industrial Engineering, J.B. Speed School of Engineering

[b]Department of Oral Health and Rehabilitation, School of Dentistry

University of Louisville, KY, 40292

REVIEWED

Abstract

Dental porcelain material is a typical glass ceramic material that is widely used in dental restoration applications. However, there still exists limited knowledge about the fabrication of this type of materials using binder jetting additive manufacturing process. There are several important factors such as saturation level, power level, drying time as well as spread speed, which would potentially affect the accuracy and strength of the printed parts before and after sintering. Therefore, in this research an extensive experimental study was performed to obtain the optimal process parameters for the dental porcelain materials fabricated via ExOne binder jetting system. The results also provide general printing guidelines for the fabrication of glass ceramic materials.

Keywords: 3D printing, Binder jetting process, green parts, sintering

Introduction

Additive Manufacturing (AM) or 3D printing (3DP) technology refers to processes in which instead of removing the extra materials from the initial block, a part is built up layer by layer using materials which are mostly available in fine powder form. Wide range of materials such as metals, ceramics, polymers, and composites could potentially be used as build material in such technology. AM technology consists of various processes such as stereolithography (SLA), selective laser sintering (SLS), binder jetting process, laminated object manufacturing (LOM),and fused deposition modeling (FDM). Binder jetting process, which was initially developed at the Massachusetts Institute of Technology, is an AM technology whereby the layer addition is realized through selective deposition of a suitable binder [1, 2]. During the process, successive 2D profiles are then printed, each time on a freshly laid layer of powder until the whole part is complete. Binder, which is deposited through a printhead, would join the respective profiles of each layer together. After completion, the printed part (green part) is baked in an oven in order to obtain enough handling strength. Thereafter, unbound powder is removed from the part and suitable post-processing is carried out such as sintering or infiltration [2]. The binder jetting process has demonstrated the capability of fabricating parts of a variety of materials, including ceramics, metals, shape memory alloys (SMA), and polymers with an array of complex geometries [3–9].

Due to its unique capability in printing parts with complicated geometries and using a wide range of built materials, binder jetting has received considerable attentions by various researchers. For instance, binder jetting process has been implemented to produce 3D porous scaffolds. This process allows tissue engineers to design and fabricate complicated scaffold shapes with controlled micro- and macro-open porosity architecture [10-12]. As another example, some researchers utilized the 3D printing binder jetting process for manufacturing of functionally graded material parts [13, 14]. However, despite its relatively straightforward work principle, the physics of binder jetting process is rather complex. There exist several adjustable parameters such as binder amount, drying power level, drying time, and powder spread speed which could potentially affect accuracy and strength of the green parts [10]. Different works have been conducted on the simulation and optimization of such parameters in this process, and new materials with better strength and performance have been used for fabrication of parts with variety of applications like those in electronics, medicine and dentistry. In [15], powder with bimodal distribution was used to improve the surface quality of the 3D printed parts. Liou et al. [16] simulated three dimensional droplet formation during inkjet printing. Stopp et al. [17] utilized a novel approach for calibration of 3D printer and consequently increment of parts accuracy. The method which they implemented was based upon the setting of bleed compensation. Dimitrov et al. [18] studied the achievable dimensional accuracy of the 3D printed parts. As a result, general international tolerance grades of the 3D printed parts produced by binder jetting process with different powders were provided by this research. Suwanprateeb and Suwanpreuk [19] fabricated transparent models similar to stereolithography models using a new composition of powder and binder via binder jetting process. Ramakrishnan et al. [20] evaluated the applicability of ceramic inks with alumina and zirconia powders in ethyl alcohol. In addition, they performed mathematical modeling and simulation with droplet formation and spread in direct ceramic inkjet printing. Pilipović et al. Also in [10] Vaezi and Chua evaluated the effects of layer thickness and binder saturation parameters on 3D printing process.

Despite the various researches in this area, so far very limited work has been focused on the investigation of various controllable printing parameters in binder jetting process, which could substantially affect accuracy and strength of the parts, and introduce deviations even before the parts undergo secondary processes. Therefore having a good understanding and scientific insight of the practical effects of such parameters on the strength and accuracy seems to be necessary. Printing parameters such as binder amount, drying power level, drying time, powder spread speed, layer thickness and powder size play an important role on the strength and accuracy of the 3D printed parts. In this study four independent adjustable factors in the binder jetting process - binder amount, the drying power level, drying time and powder spread speed - are considered to evaluate their effects on the strength and accuracy of the printed green parts.

Methodology

For this research, off-the-shell dental porcelain was used, which is a commerical product for artificial dental restorations such as crowns, veneers and onlays. Table 1 shows the composition of the porcelain used in this research.

Table 1. Chemical composition of used dental porcelain

SiO_2 %	Al_2O_3 %	K_2O %	Na_2O %
55-61	13-16	11-15	4-6

The original powder exhibits significant aggregation, which makes it difficult to spread uniformly in the printing process. From the SEM microscopy, the porcelain particles have irregular shapes and different sizes ranging from 0.3-10 μm (figure 1). It was previously found that the irregular morphology and large particle size range significantly reduces the powder flowability [21]. In order to improve the flowability of the powder, a flow agent was added to the porcelain powder. The function of the flow agent is believed to be analogous to the addition of sand between two surfaces, which serves as low friction contact media and therefore reduces the resistance of relative motions between the powder particles. The flow agent chosen was Aerosil R 972 Hydrophobic fumed silica powder (COSMOS Plastic & Chemicals), with an average particle size of 16 nm. This powder is composed of 99.8% fumed silica after treated with dimethyldichlorosilane (DDS) based on a hydrophilic fumed silica with a specific surface area of 130 m^2/g (Aerosil R 972 MSDS). Up to 10% volume percentage flow agent was measured and added to the original porcelain powder, and the container with the mixture was shaken by hand until well-proportioned mixed powder was visually discernable.
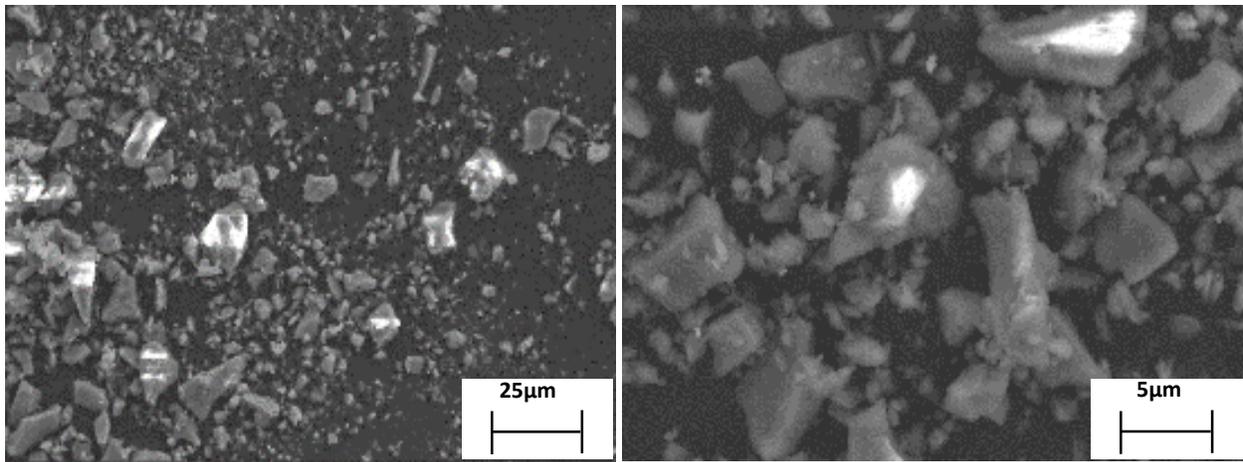

Fig. 1 Morphology of the original powder in SEM

For this research, the ExOne M-Lab machine was utilized in order to print the samples This process starts with spreading the first layer on the build plate. After the initial heating of the first layer, a printhead selectively deposits the binder on the specific regions. Thereafter, binder infiltrates into the powder bed and bonds the powder particles to create geometries. After the printing operation of each layer, the powder bed is heated by an infrared heater for a set amount of time in order to partially cure the binder and to give the printed area necessary strength for consequent printing. For each new layer, the powder is fed from the powder feeding chamber via a roller. The procedures are repeated until the parts are complete. The schematic of the ExOne 3DP process is shown in Fig. 2.
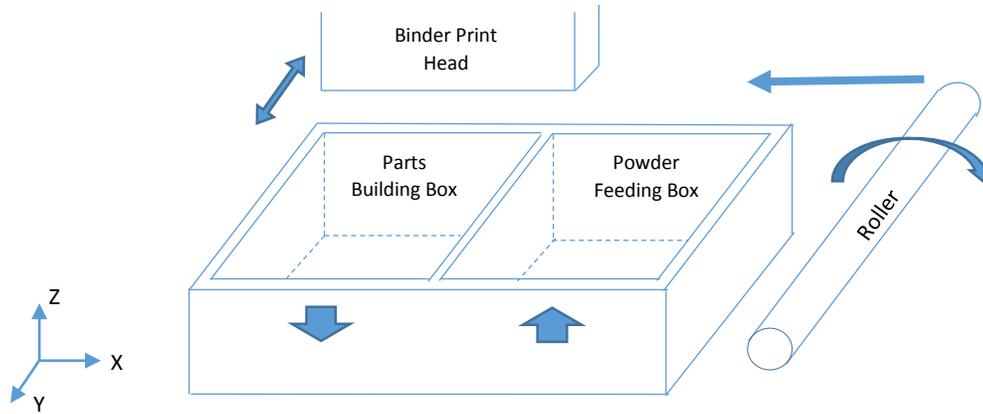
Fig 2. Schematic of binder jetting process for the ExOne M-Lab machine [22]

In binder jetting process, four adjustable parameters considered in this study are defined as follows:

Saturation level is amount of the binder which is deposited through printhead. It is a measurement of the theoretical percentage of void space (V_{air}) in the print material that is filled with binder (V_{binder}). The saturation ratio is determined from Equations (1) and (2), and is based on the packing density of the powder bed (PR) and the volume of a defined envelope ($V_{envelope}$). The ExOne M-Lab printing software calculates the required volume of binder to be printed once the desired binder saturation and packing density of the powder are input by the user. It is worth mentioning that packing density specifies how much void space exists in the print material after spreading. For dental porcelain which was used for this study, the packing density was 40%.

Desired saturation level = V_{binder} / V_{air} (1)

$V_{air} = (1 - \frac{PR}{100}) * V_{envelope}$ (2)

Power level is defined as the intensity of applied heat using infrared heater; drying time is an amount of time considered for drying of the deposited binder, and finally spread speed is the rate by which the powder is spread.

Since in the M-Lab machine, the binder saturation level is a the hard-to-change process parameter, split-plot design was chosen to be used for conducting the experiments, saturation level as a hard-to-change factor and power level, drying time, and spread speed as easy-to-change factors. Table 2 shows the levels of the factors which were considered for this study.

Table 2: Factors and levels of the experiment

Factors	Saturation level (%)	Power level (%)	Drying time (s)	Spread speed (mm/s)
Levels	50, 75	45, 60, 75	30, 45, 60	2, 6

A full factorial experimental design with a total of 2*3*3*2 = 36 experiments were conducted. Four cubic specimens with the size of 10x10x10 mm were printed out under different combinations of factors levels. Afterwards, the fabricated green parts were put into a drying oven

and baked at 200°C for 2.5 hours to fully cure the binder. Fig. 3 shows the samples after curing printed with saturation level of 75%, power level of 45%, drying time of 30 s, and spread speed of 2 mm/s.

Fig 3. Parts after curing for 2.30 hour at 200°C

After the green parts were cleaned, their dimensions were measured using a digital caliber, and their strength was evaluated through compressive testing performed on a Shimadzu micro-tensile testing machine. Fig. 4 shows a sample under compressive test.
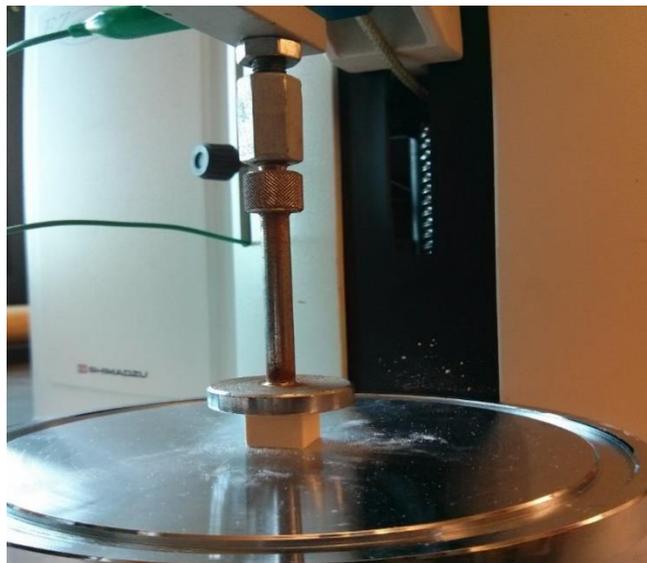

Fig 4. A sample under compressive test

After removing the extra powder, the green parts need to be sintered to achieve the desired strength and density. The general firing schedule for dental porcelain ceramic used in this study is shown in Fig. 5. Based upon previous researches [14, 21, 22] with the sintering parameters, the temperature and holding time that results in the best densification and strength for dental

porcelain parts are 900 °C and 1 minute, respectivelytime. In this firing schedule, parts are heated to 500 °C with a set rate of 10 °C/min and held at this temperature for 0.5 hour to completely burn out the binder. After this step the parts are heated to 900 °C with a heating rate of 10 °C/min and held in this temperature for 1 minute, and then cooled at 10°C/min to room temperature.

ANOVA (Analysis of variance) was implemented to analyze the experimental data. Residual analysis from Minitab software proved that this method is a suitable procedure for analyzing the experimental data.
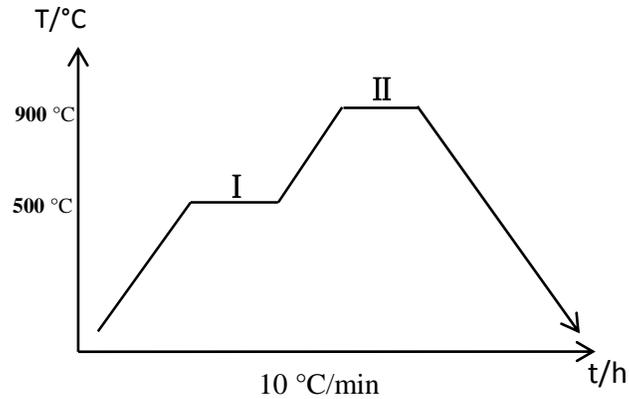

Fig 5. Firing schedule

Results and discussion

Green parts

Accuracy in Z direction

Fig. 6 shows the effects of the different parameters and their interactions on accuracy of the printed parts in z direction (perpendicular to build plate). Based on ANOVA, power level, spread speed and drying time have significant effects on part accuracy, while the effect of the power level is more significant than other factors. A high heating power cures the deposited binder before it completely join the particles in the specified design area, whilst with a low heating power some binder remains insufficiently cured, which consequently results in part accuracy deterioration. Moreover, from Fig. 6 it is clear that increasing the saturation level from 50% to 75% does not appear to have significant effect on the accuracy of the parts. Another important fact which could be inferred from the results is that when power level is not sufficient to cure the binder, increasing drying time would help the accuracy. However, when the infrared heater is set to enough power to cure the binder before spreading the next layer and subsequently binder, increasing drying time could negatively affect the accuracy. Similarly, if power level starts to exceed the right amount, increasing the drying time would decrease the part accuracy. In this situation, higher drying time would over-cure the binder which results in week bonds between the successive layers, and consequently less accurate parts.

From the results, powder spread speed appeared to have less significant effect than other parameters. Lower spread speed is always desired for uniform powder spreading and therefore the quality of printed parts. However, it could significantly increase the printing time. Therefore,

if speed of spreading exceeds the threshold, it will reduce the part quality in terms of both accuracy and strength. As a general role finer particles require a relatively slower spread speed, whereas relatively higher spread speed could be set for coarse particles [24].

Based upon data analysis, the appropriate parameters to obtain the best accuracy in the z direction is the 50% percent saturation level, 60% power level, 2 mm/s for spread speed and 60s for drying time.
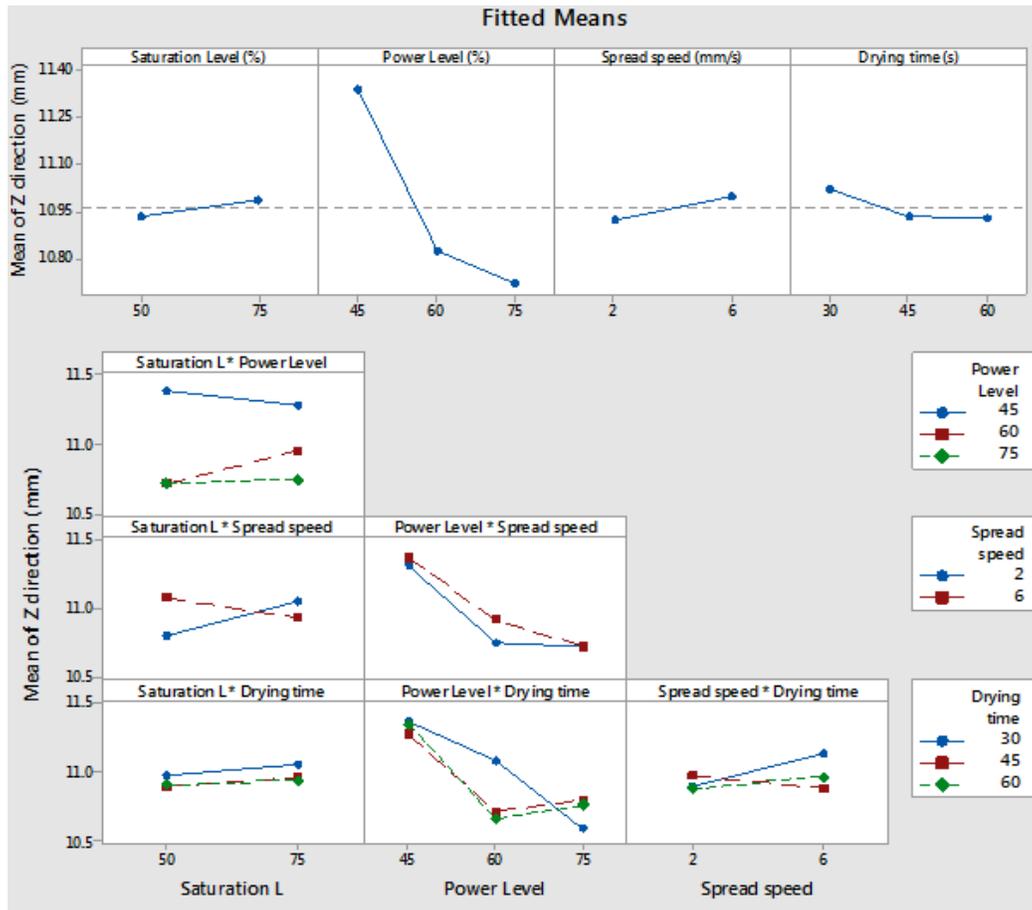

Fig 6. Effect of factors and their interaction on part accuracy in z direction

Accuracy in X direction
It was realized that the geometrical accuracies in the X direction (direction along which roller travels) and the Y direction (direction normal to the roller travel direction) are different. Therefore the accuracies at both directions were investigated. After printing the parts, it was observed that dimensions of the top section (top layers) of some parts vary with those of the bottom section (bottom layers which are printed earlier in the process). Fig. 7 shows a general trend observed in such printed parts. This phenomena happens when the power level or drying time is not sufficient to cure the binder sufficiently. In this case, printing successive layers on top of under-cured binder would decrease accuracy in bottom section of the part more than top layers (which are printed later in the process) probably due to gradually accumulated weights from the top layers. In order to investigate the degree of part distortion, two measurements, top section and bottom section, were conducted for evaluating the accuracy in the X direction for all the printed parts.

Fig. 8 and 9 show that how different parameters and their interactions affect the accuracy of the printed parts in the x direction. From the results, effect of the parameters and their interactions on accuracy is the same for the both top and bottom sections. However, the top section dimensions are more accurate than those of the bottom sections as expected.

In addition, it was previously observed that increasing spread speed would decrease the accuracy in Z direction. However, as shown in Fig. 8 and 9, effect of powder spread speed on accuracy of the parts in X direction is less significant.

Another noticeable fact that could be concluded from Fig 8 and 9 is the different effect of the drying time on top and bottom section. Increasing drying time would continually increase the accuracy of the parts on bottom section. However, for the top section, increasing this parameter first increases and then decreases the part accuracy, which again may be contributed to the over-curesof the binder. Based upon ANOVA results, in order to achieve the best accuracy in X direction saturation level of 50%, power level of 75%, spread speed of 6 mm/s, and drying time of 60s would be optimal. Comparing the results of accuracy in Z and X directions shows that spread speed and power level factors affect differently on accuracy in Z and X directions. In other words, to obtain the better accuracy in z direction, the spread speed should be decreased. However, in order to reach the optimal accuracy in X direction spread speed has to be increased. Although higher power level would reduce binder permeation in X and Y direction after depositing and consequently would increase accuracy, due to over-curing of binder and weak bond between successive layers the part accuracy in the z direction would decrease.

It is worth mentioning that effect of the factors and their interactions on accuracy of the green parts in Y direction are the same as those in X direction. ANOVA demonstrate that 50% saturation level, 75% power level, 6 mm/s spread speed, and 60s drying time are indeed optimal levels of factors for part accuracy in both X and Y directions as expected.
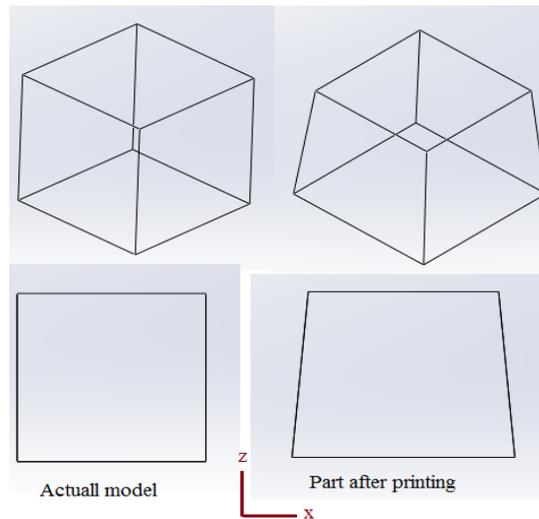

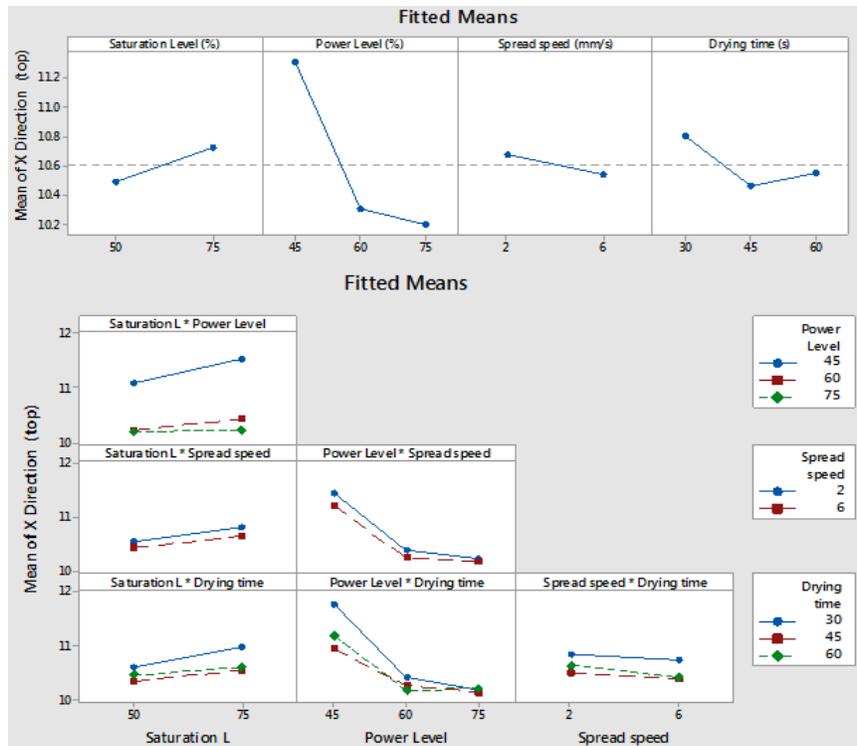Fig 7. General shape of the parts after printing

Fig 8. Effect of different factors and their interaction on part accuracy in x direction (top surfaces)
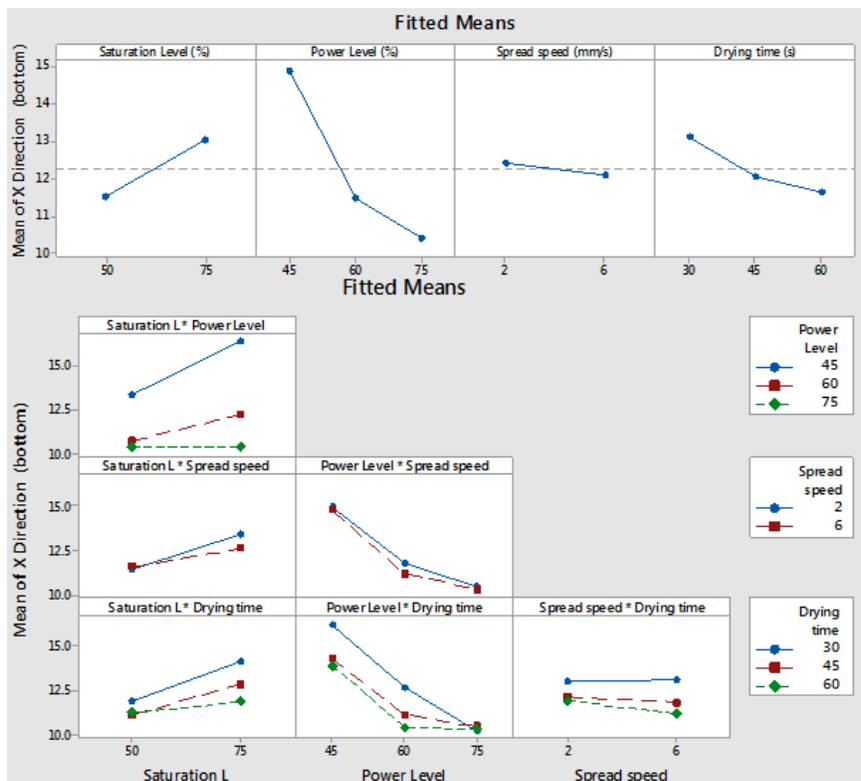

Fig 9. Effect of different factors and their interaction on part accuracy in x direction (bottom surfaces)

Green part strength

The factors and their interactions show different trends of effects for green part strength. Fig. 12 shows how they influence green part strength. As shown from the figure, increasing saturation level from 50% to 75% would increase part strength by 50%. This can be readily explained that with higher saturation level, more binder would penetrate in vertical and lateral directions over the surface and, as a result, creates better bonding between particles and between layers.

On the other hand, the green part strength decreases significantly with increasing spread speed and drying time. As mentioned earlier, increasing spread speed would decrease the powder uniformity and packing density of spread powder, and as a result, will decrease the part strength in the green state. Also the more drying time over-cures the binder before spreading the next layer resulting in a weak interface bond between layers and less sufficient wetting between powder particle, which consequently result in less strong green parts.

Furthermore, although increasing the power level from 45% to 60% increases the strength from 55N to 95N (73% increase), further increasing from 60% to 75% decreases the green part strength by 58%, which again could be contributed to the different curing conditions of the binder. Also, the influence of each individual factor should be considered in conjunction with other factors since the interactions of the factors also significantly affect the strength. Fig. 13 shows the surface plot of strength in terms of saturation level and drying time interaction. As it could be concluded from this figure, the power level and time for drying the binder should be selected in such a way that the sprayed binder is dried at an optimal condition. The higher the power level is set, the less the drying time would be required. In addition, Fig. 12 demonstrates that if the saturation level is increased to obtain better strength, the power level and drying time are to be adjusted accordingly to get reasonable accuracy and strength.

Contour plot of strength versus saturation level and spread speed is shown in Fig. 14. From the figure it is clear that when the saturation level is increased, it is necessary to decrease the spread speed in order to get the optimal strength. In other words, at higher saturation levels the effect of spread speed factor on strength of the green part is more significant.

From ANOVA analysis, the two setting scenarios that could result in optimal green part strength could be determined as:

1. Saturation level of 75%, Power level of 60%, Drying time of 60s and Spread speed of 2 mm/s or
2. Saturation level of 75%, Power level of 75%, Drying time of 30s and Spread speed of 2 mm/s

Either one the above settings could result in high green part strength. It is worth mentioning that in setting 2 if the drying is increased from 30s to 45s, ANOVA result shows that strength of the printed parts would decrease by 66% due to over-cured binderas explained previously.
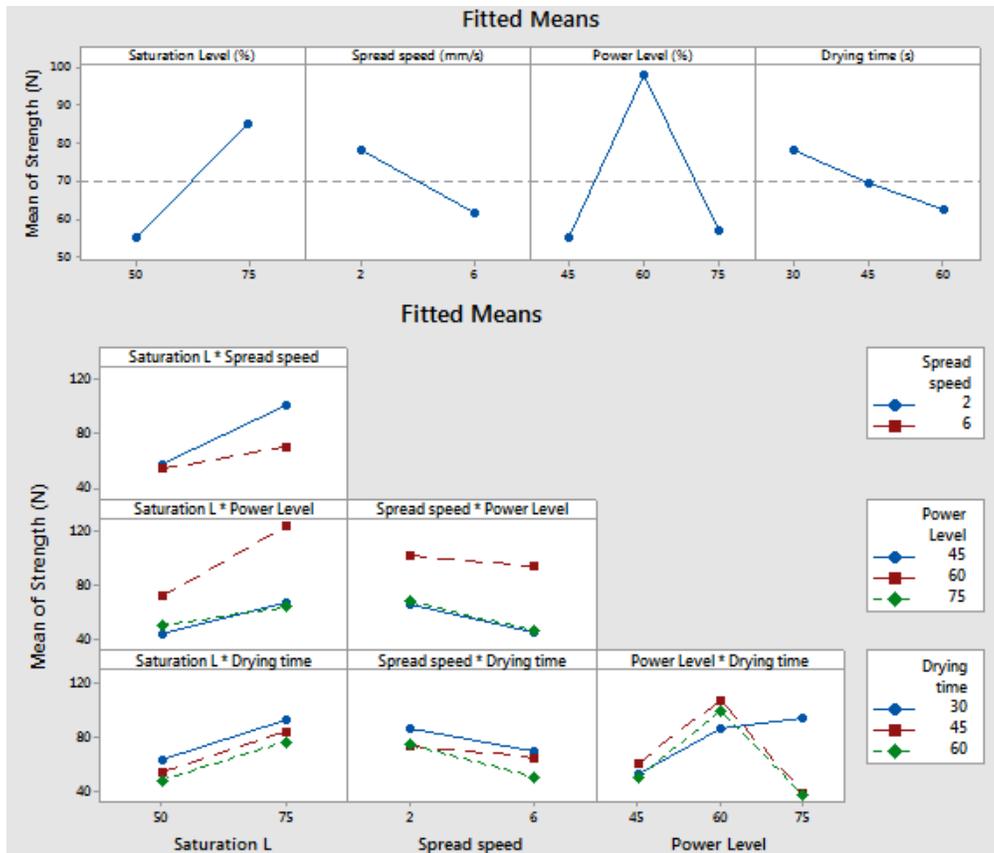
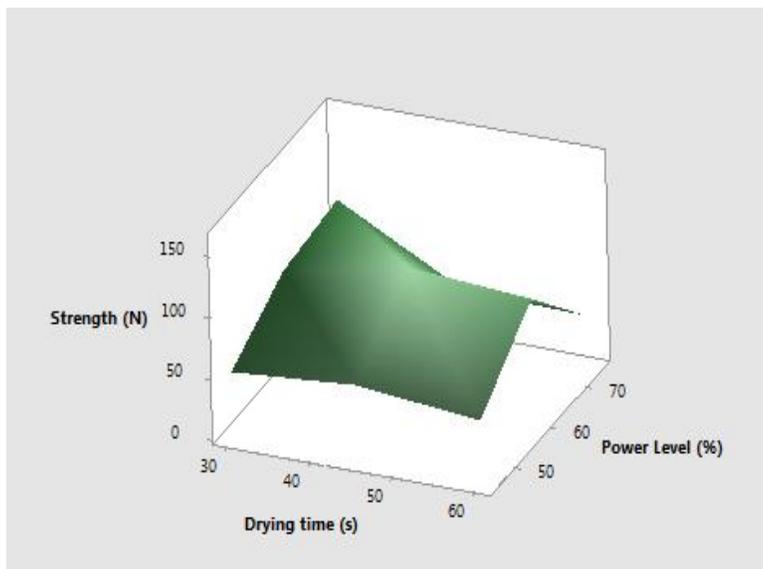Fig 12. Effect of different factors and their interaction on green part strength

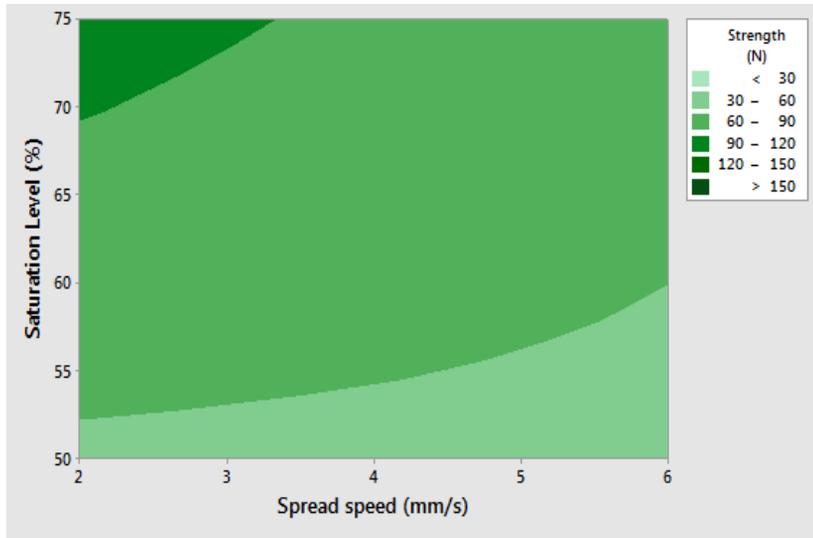Fig 13. Surface plot of green part strength vs drying time and power level

Fig 14. Contour plot of green part strength vs saturation level and spread speed

Sintered parts

Shrinkage in Z direction

For shrinkage calculations, dimensions of the green parts were used as the reference bases. ANOVA results for the shrinkage of the parts after sintering in Z direction have been shown in Fig. 15. As could be observed, only spread speed and its interaction with saturation level have significant effects on shrinkage. Fig. 16 and 17 show their effects on part shrinkage. From Fig. 16 it is obvious that higher spread speed will increase the shrinkage and therefore decrease the part accuracy after sintering, which is likely to be contributed by the decrease of packing density and uniformity of the spread powder as explained earlier. Also based on Fig. 17, at 50% binder saturation changing spread speed from 2 mm/s to 6 mm/s could significantly affect the shrinkage. However, at 75% saturation level the spread speed does have considerable effect, which might be a result of the surface tension driven hydrodynamic clumping created by excessive amount of liquid.

```
Source                                                              P-Value
  Saturation Level (%)                                                0.133
  Spread speed (mm/s)                                                 0.005
  Power Level (%)                                                     0.186
  Drying time (s)                                                     0.364
  Saturation Level (%)*Spread speed (mm/s)                            0.034
  Saturation Level (%)*Power Level (%)                                0.219
  Saturation Level (%)*Drying time (s)                                0.097
  WP(Saturation Level (%))                                            0.604
  Spread speed (mm/s)*Power Level (%)                                 0.286
  Spread speed (mm/s)*Drying time (s)                                 0.169
  Power Level (%)*Drying time (s)                                     0.298
  Saturation Level (%)*Spread speed (mm/s)*Power Level (%)            0.600
  Saturation Level (%)*Spread speed (mm/s)*Drying time (s)            0.289
  Saturation Level (%)*Power Level (%)*Drying time (s)                0.115
  Spread speed (mm/s)*Power Level (%)*Drying time (s)                 0.183
  Saturation Level (%)*Spread speed (mm/s)*Power Level (%)*Drying time (s)   0.183
```

Fig 15. ANOVS result for shrinkage in Z direction after sintering

Fig 16. Effect of spread speed on shrinkage in Z direction
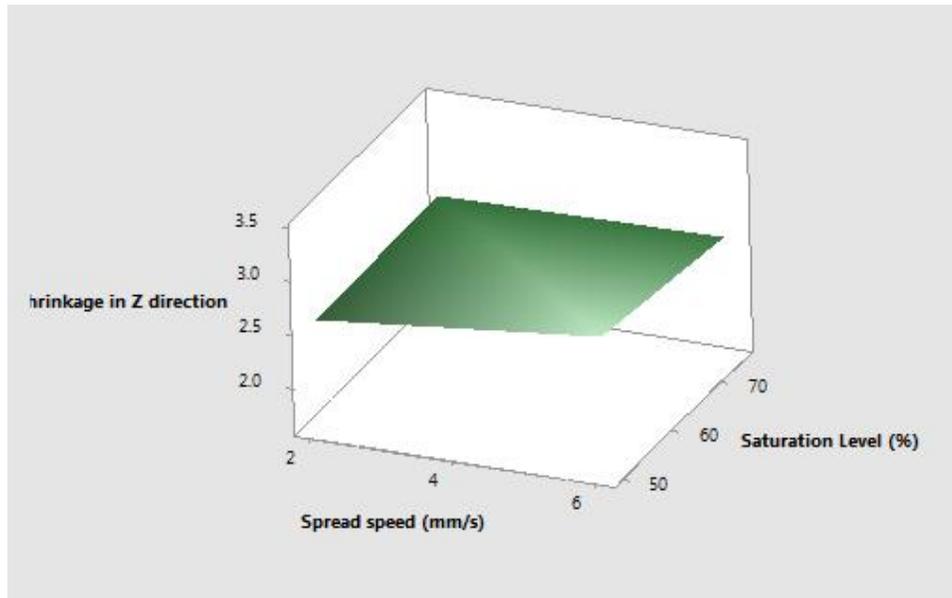
Fig 17. Effect of spread speed and saturation level interaction on shrinkage in Z direction

Shrinkage in X direction (top & bottom)

ANOVA results for shrinkage of the sintered parts in X direction (top section) have been shown in Fig. 18. As expected, the only factor which significantly affects the part shrinkage is spread speed. Fig. 19 demonstrates how changing spread speed would affect the shrinkage of the parts in the X direction. In addition, ANOVA results for shrinkage of sintered parts for the bottom section are shown in Fig. 20 and 21, which also show that spread speed is the only significant factor that affects the part shrinkage in the X direction. Since increasing the spread speed affects the packing density and uniformity of the spread powder, higher spread speed will increase the shrinkage and therefore decrease the part accuracy after sintering.

```
Source                                                                   P-Value
  Saturation Level (%)                                                     0.096
  Spread speed (mm/s)                                                      0.000
  Power Level (%)                                                          0.073
  Drying time (s)                                                          0.100
  Saturation Level (%)*Spread speed (mm/s)                                 0.414
  Saturation Level (%)*Power Level (%)                                     0.382
  Saturation Level (%)*Drying time (s)                                     0.124
  WP(Saturation Level (%))                                                 0.374
  Spread speed (mm/s)*Power Level (%)                                      0.129
  Spread speed (mm/s)*Drying time (s)                                      0.928
  Power Level (%)*Drying time (s)                                          0.196
  Saturation Level (%)*Spread speed (mm/s)*Power Level (%)                 0.197
  Saturation Level (%)*Spread speed (mm/s)*Drying time (s)                 0.281
  Saturation Level (%)*Power Level (%)*Drying time (s)                     0.106
  Spread speed (mm/s)*Power Level (%)*Drying time (s)                      0.319
  Saturation Level (%)*Spread speed (mm/s)*Power Level (%)*Drying time (s) 0.082
```

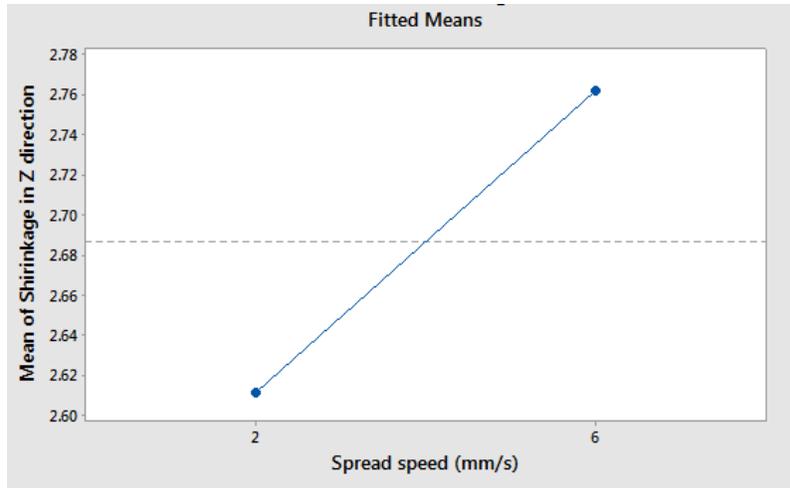Fig 18. ANOVA results on part shrinkage in X direction (top section)
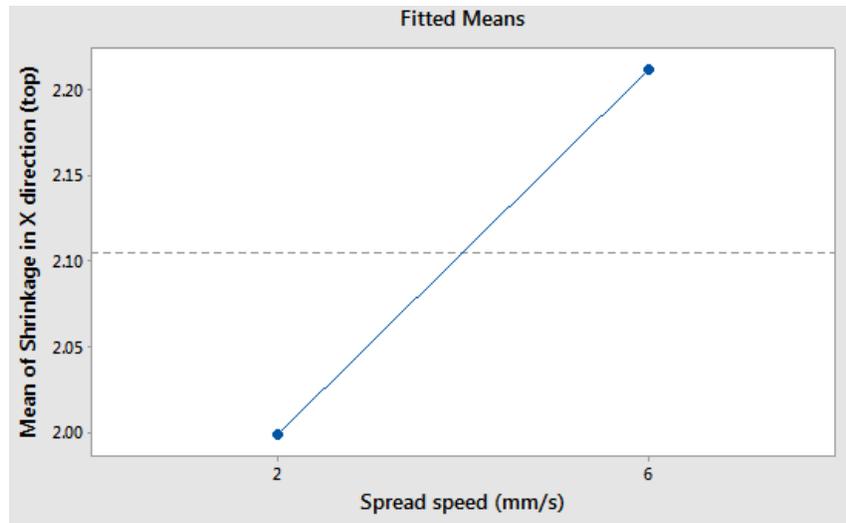
Fig 19. Spread speed effect on shrinkage in X direction (top section)

```
Source                                                                   P-Value
  Saturation Level (%)                                                     0.486
  Spread speed (mm/s)                                                      0.000
  Power Level (%)                                                          0.129
  Drying time (s)                                                          0.505
  Saturation Level (%)*Spread speed (mm/s)                                 0.980
  Saturation Level (%)*Power Level (%)                                     0.161
  Saturation Level (%)*Drying time (s)                                     0.982
  WP(Saturation Level (%))                                                 0.324
  Spread speed (mm/s)*Power Level (%)                                      0.824
  Spread speed (mm/s)*Drying time (s)                                      0.239
  Power Level (%)*Drying time (s)                                          0.577
  Saturation Level (%)*Spread speed (mm/s)*Power Level (%)                 0.868
  Saturation Level (%)*Spread speed (mm/s)*Drying time (s)                 0.441
  Saturation Level (%)*Power Level (%)*Drying time (s)                     0.812
  Spread speed (mm/s)*Power Level (%)*Drying time (s)                      0.537
  Saturation Level (%)*Spread speed (mm/s)*Power Level (%)*Drying time (s) 0.943
```

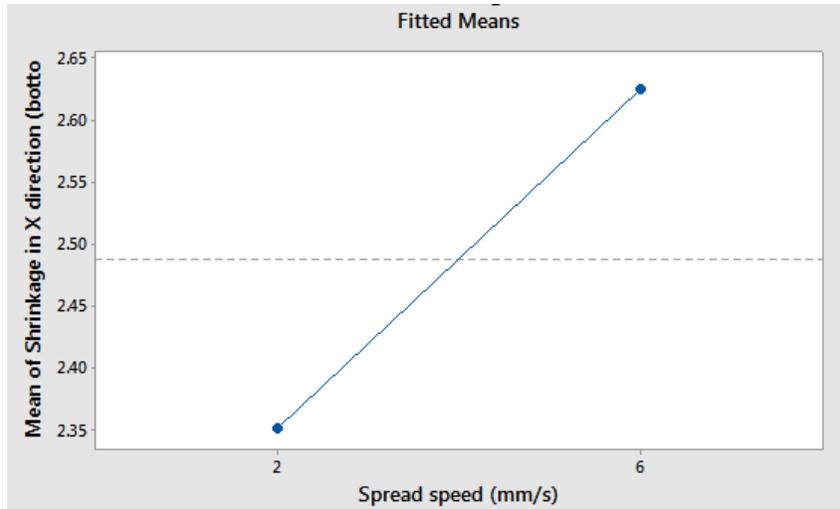Fig 20. ANOVA results on part shrinkage in X direction (bottom section)

Fig 21. Spread speed effect on shrinkage in X direction (bottom section)

Shrinkage in Y direction (top & bottom)

As Fig. 22 and 24 show, for the case of shrinkage in Y direction for both top and bottom sections, the spread speed parameter is still the most significant factor influencing the part shrinkage after sintering, which exhibit the same trend as the direction as shown in Fig. 23 and 25.

```
Source                                                                  P-Value
  Saturation Level (%)                                                    0.477
  Spread speed (mm/s)                                                     0.001
  Power Level (%)                                                         0.101
  Drying time (s)                                                         0.263
  Saturation Level (%)*Spread speed (mm/s)                                0.231
  Saturation Level (%)*Power Level (%)                                    0.273
  Saturation Level (%)*Drying time (s)                                    0.225
  WP(Saturation Level (%))                                                0.051
  Spread speed (mm/s)*Power Level (%)                                     0.328
  Spread speed (mm/s)*Drying time (s)                                     0.013
  Power Level (%)*Drying time (s)                                         0.254
  Saturation Level (%)*Spread speed (mm/s)*Power Level (%)                0.128
  Saturation Level (%)*Spread speed (mm/s)*Drying time (s)                0.109
  Saturation Level (%)*Power Level (%)*Drying time (s)                    0.367
  Spread speed (mm/s)*Power Level (%)*Drying time (s)                     0.101
  Saturation Level (%)*Spread speed (mm/s)*Power Level (%)*Drying time (s)  0.202
```

Fig 22. ANOVA results on part shrinkage in Y direction (top section)

Fig 23. ANOVA results on part shrinkage in Y direction (top section)

```
Source                                                                   P-Value
  Saturation Level (%)                                                     0.312
  Spread speed (mm/s)                                                      0.045
  Power Level (%)                                                          0.300
  Drying time (s)                                                          0.129
  Saturation Level (%)*Spread speed (mm/s)                                 0.091
  Saturation Level (%)*Power Level (%)                                     0.108
  Saturation Level (%)*Drying time (s)                                     0.447
  WP(Saturation Level (%))                                                 0.323
  Spread speed (mm/s)*Power Level (%)                                      0.139
  Spread speed (mm/s)*Drying time (s)                                      0.144
  Power Level (%)*Drying time (s)                                          0.131
  Saturation Level (%)*Spread speed (mm/s)*Power Level (%)                 0.103
  Saturation Level (%)*Spread speed (mm/s)*Drying time (s)                 0.324
  Saturation Level (%)*Power Level (%)*Drying time (s)                     0.211
  Spread speed (mm/s)*Power Level (%)*Drying time (s)                      0.078
  Saturation Level (%)*Spread speed (mm/s)*Power Level (%)*Drying time (s) 0.519
Error
Total
```
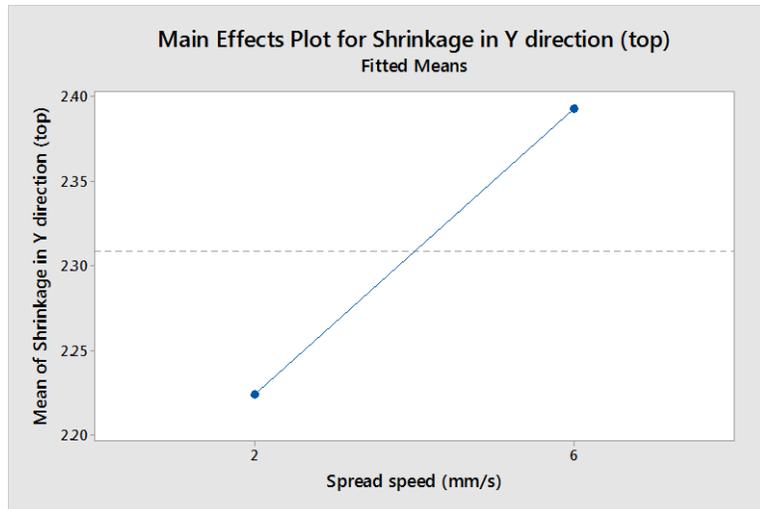
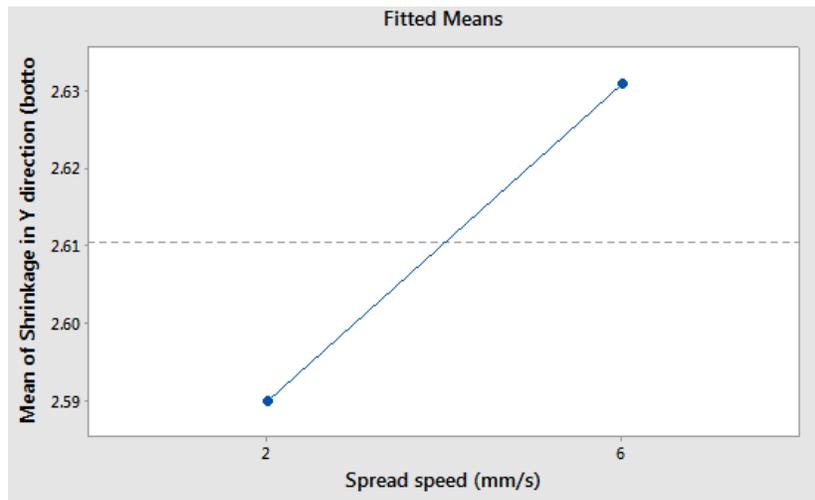Fig 24. ANOVA results on part shrinkage in Y direction (bottom section)

Fig 25. Spread speed effect on shrinkage in Y direction (bottom section)

Conclusion

In this research an extensive experimental study was conducted in an attempt to assess the effect of various printing parameters on part accuracy and strength, which include the binder amount, the drying power, drying time and powder spread speed. The results could be summarized as follows:

1) Effect of the power level on accuracy of green parts in Z direction is more significant than other factors. Increasing the power level from 45% to 75% increases the part accuracy. Also increasing the spread speed would slightly decrease the green part accuracy in Z direction; and increasing the saturation level from 50% to 75% does not appear to have significant effect on the accuracy of the parts. The appropriate parameters to obtain the best accuracy in the z direction is the 50% percent saturation level, 60% power level, 2 mm/s for spread speed and 60s for drying time.

2) Increasing spread rate from 2 mm/s to 6 mm/s would increase the accuracy of the green part in X direction. Increasing drying time would continually increase the accuracy of the parts on bottom section. However, for the top section, the increase of drying time would first increase and then decrease the part accuracy. In order to reach the optimal accuracy in X direction spread speed should be increased. Also greater power level would increase accuracy. In order to acquire the best accuracy in X direction saturation level of 50%, power level of 75%, spread speed of 6 mm/s, and drying time of 60s would be necessary.

3) Effect of the parameters and their interactions in Y direction are the same as their effects in X direction. Results suggest that 50% saturation level, 75% power level, 6 mm/s spread speed, and 60s drying time are indeed optimal levels of factors for part accuracy in both X and Y directions.

4) Increasing saturation level from 50% to 75% would increase green part strength by 50%. Moreover, the green part strength decreases significantly with increasing spread speed and drying time. Furthermore, the increase of the power level from 45% to 60% increases the strength 55N to 95N which equals to an 73% improvement, while further increase from 60% to 75% decreases the green part strength by 58%. As general rule, the higher the power level is chosen, the less the drying time would be required. If the saturation level is increased to obtain better strength, the power level and drying time are to be adjusted accordingly to get reasonable accuracy and strength. In order to obtain the optimal green part strength either one of following settings could be selected for printing of dental porcelain ceramics:

   1. Saturation level of 75%, Power level of 60%, Drying time of 60s and Spread speed of 2 mm/s or
   2. Saturation level of 75%, Power level of 75%, Drying time of 30s and Spread speed of 2 mm/s

5) For the shrinkage of the parts after sintering for all direction (Z, X, and Y) the only significant factor is spread speed parameter as expected. In all cases increasing spread speed increase the part shrinkage.

Acknowledgement

References

[1] M. Cima, E. Sachs, T.L. Fan, J.F. Bredt, S.P. Michaels, S. Khanuja, A. Lauder, S.J. Lee, D. Brancazio, A. Curodeau, H. Tuerck, United States Patent No. 5387380 (1995).

[2] E.M. Sachs, M. Cima, P. Williams, D. Brancazio, J. Cornie, Trans. ASME, Ser. B 114 (1992) 481.

[3] Seitz H, RiederW IS, Leukers B, Tille C (2005) Threedimensional printing of porous ceramic scaffolds for bone tissue engineering. J Biomed Mater Res 74B:782–788

[4] Noguera R, Lejeune M, Chartier T (2005) 3D fine scale ceramic components formed by ink-jet prototyping process. J Eur Ceram Soc 25:2055–2059

[5] Lejeune M, Chartier T, Dossou-Yovo C, Noguera R (2009) Ink-jet printing of ceramic micro-pillar arrays. J Eur Ceram Soc 29:905–911

[6] Cawley JD (1999) Solid freeform fabrication of ceramics. Curr Opin Solid State Mater Sci 4:483–489

[7] Vorndran E, Klammert U, Klarner M, Grover LM, Barralet JE, Gbureck U (2009) 3D printing of β-tricalcium phosphate ceramics. Dent Mater 25:e18–e19

[8] Cappi B, Özkol E, Ebert J, Telle R (2008) Direct inkjet printing of Si3N4: characterization of ink, green bodies and microstructure. J Eur Ceram Soc 28:2625–2628

[9] Lu K, Reynolds WT (2008) 3DP process for fine mesh structure printing. Powder Technol 187:11–18

[10] Mohammad Vaezi & Chee Kai Chua (2010) Effects of layer thickness and binder saturation level parameters on 3D printing process. Int J Adv Manuf Technol (2011) 53:275–284

[11] Lam CXF, Mo XM, Teoh SH, Hutmacher DW (2002) Scaffold development using 3D printing with a starch-based polymer. Mater Sci Eng C 20:49–56

[12] Yeong WY, Chua CK, Leong KF, Chandrasekaran M, Lee MW (2006) Indirect fabrication of collagen scaffold based on inkjet printing technique. Rapid Prototyping J 12:229–237

[13] Chiu WK, Yu KM (2008) Direct digital manufacturing of threedimensional functionally graded material objects. Comput Aided Des 40:1080–1093

[14] Hadi M, Li Y, Shanshan Zh, Amir A. Z, A preliminary study of the graded dental porcelain ceramic structures fabricated via binder jetting 3D printing, Proceedings of the 24th International Solid Freeform Fabrication Symposium. Austin, TX, USA. 2014

[15] Lanzetta M, Sachs E (2003) Improved surface finish in 3D printing using bimodal powder distribution. Rapid Prototyping J 9:157–166

[16] Liou TM, Shih KC, Chau SW, Chen SC (2002) Threedimensional simulations of the droplet formation during the inkjet printing process. Int Commun Heat Mass Transf 29:1109–1118

[17] Stopp S, Wolff T, Irlinger F, Lueth T (2008) A new method for printer calibration and contour accuracy manufacturing with 3Dprint technology. Rapid Prototyping J 14:167–172

[18] Dimitrov D, Wijck WV, Schreve K, de Beer N (2006) Investigating the achievable accuracy of three dimensional printing. Rapid Prototyping J 12:42–52

[19] Suwanprateeb J, Suwanpreuk W (2009) Development of translucent and strong three dimensional printing models. Rapid Prototyping J 15:52–58

[20] Ramakrishnan N, Rajesh PK, Ponnambalam P, Prakasan K (2005) Studies on preparation of ceramic inks and simulation of drop formation and spread in direct ceramic inkjet printing. J Mater Process Technol 169:372–381

[21] Li Yang, Shanshan Zhang, Gustavo Oliveira, Brent Stucker, Development of a 3D Printing Method for Production of Dental Application. Proceedings of the 24th International Solid Freeform Fabrication Symposium. Austin, TX, USA. 2013.

[22] Shanshan Z, Hadi M, Li Y, Amir A. Z, J.J.S. Dilipa and Brent S, An Experimental Study of Ceramic Dental Porcelain Materials Using A 3D Print (3DP) Process, Proceedings of the 24th International Solid Freeform Fabrication Symposium. Austin, TX, USA. 2014.

[23] M. Schmid, G. Levy, F. Amado, K. Wegener, Flowability of Powders for Selective Laser Sintering (SLS) investigated by Round Robin Test, International Conference on Advanced Research in Virtual and Rapid Prototyping, 2013, Leiria, Portugal, ISBN 978-1-138-00137-4, Pages 95-99.

[24] Solaiman T, Vamsi K. B, Neal M. D., Amit B, Susmita B, Microwave Sintered 3D Printed Tricalcium Phosphate Scaffolds for Bone Tissue Engineering, J Tissue Eng Regen Med. 2013 Aug; 7(8): 631–641.